Organic μ cavities based on thermally evaporated TeO x - LiF distributed Bragg reflectors

M. Anni, G. Gigli, R. Cingolani, S. Patanè, A. Arena, and M. Allegrini

---

Articles you may be interested in

Efficiency enhancement and angle-dependent color change in see-through organic photovoltaics using distributed Bragg reflectors
Appl. Phys. Lett. **108**, 103902 (2016); 10.1063/1.4943654

Strong coupling in high-finesse organic semiconductor microcavities
Appl. Phys. Lett. **83**, 5377 (2003); 10.1063/1.1637146

Dichroic Bragg reflectors based on birefringent porous silicon
Appl. Phys. Lett. **78**, 3887 (2001); 10.1063/1.1378045

Erratum: "Distributed Bragg reflectors based on AlN/GaN multilayers" [Appl. Phys. Lett. 74, 1036 (1999)]
Appl. Phys. Lett. **74**, 4070 (1999); 10.1063/1.123264

Distributed Bragg reflectors based on AlN/GaN multilayers
Appl. Phys. Lett. **74**, 1036 (1999); 10.1063/1.123447

Organic μ cavities based on thermally evaporated TeO$_x$-LiF distributed Bragg reflectors

M. Anni,[a] G. Gigli, and R. Cingolani
National Nanotechnology Laboratory (NNL) of INFM, Dipartimento Ingegneria dell'Innovazione, Università di Lecce, Via per Arnesano, 73100 Lecce, Italy

S. Patanè and A. Arena
Istituto Nazionale Fisica per Materia (INFM), Dipartimento Fisica della Materia e Tecnologie Fisiche Avanzate, Università di Messina, Salita Sperone 31, 98166 Sant'Agata-Messina, Italy

M. Allegrini
Istituto Nazionale di Fisica per la Materia e Dipartimento di Fisica, Università di Pisa, Via F. Buonarroti n. 2 Pisa, Italy

We report on the realization of high-quality organic microcavities consisting of distributed Bragg reflectors based on lithium fluoride (LiF) and tellurium dioxide (TeO$_x$) deposited by thermal evaporation. The materials are transparent in the range of 350 nm–5 μm and have an evaporation temperature of about 1000 K. The large difference in the refractive index (about 0.9 in the visible and near-infrared range) allows one to obtain reflectivity higher than 99% over a spectral region about 200 nm wide with a small number of periods. The mirror deposition technique is suitable for the fabrication of organic quantum microcavities in a single deposition process. Three fully evaporated organic λ cavities with Phyrrometene 580 as the active material are described. The cavities show a Q value of up to 300, good uniformity, and reproducibility. © *2001 American Institute of Physics.* [DOI: 10.1063/1.1398323]

Organic semiconductors have recently attracted much attention for application in electroluminescent devices such as light emitting diodes (LEDs) and displays. Within this framework organic microcavity structures have demonstrated their utility to obtain full control of the emission energy, linewidth, intensity, and directionality of LEDs[1–9] as well as to obtain optical feedback in laser resonators.[10,11] The commonly studied organic microcavities are realized by cladding the active material between a distributed Bragg reflector (DBR) and an evaporated metallic mirror,[11–15] or by high temperature mechanical pressing of two half DBR cavities.[16] Moreover, in order to have a single μ-cavity resonance, the cavity needs a DBR that has a stop band wider than the luminescence of the organic (typically hundreds of nanometers). To satisfy such requirements DBRs of materials with a high refractive index difference must be used. To date, many different techniques and many different materials have been used for wide bandwidth DBR deposition, such as SiO$_2$–Si$_x$N$_y$ by plasma enhanced chemical vapor deposition (PECVD),[8,12–14] CF–CF(Au) by sputtering,[17] and MgF$_2$–ZrO$_2$ by laser induced vapor deposition.[18] These techniques cannot be used in the presence of an organic active material, thus requiring a complicated multistep process for realization of the cavity.

In this letter we report on the realization of DBR dielectric mirrors entirely based on low cost thermal evaporation of lithium fluoride (LiF) as the low refractive index material and tellurium oxide (TeO$_x$) as the high refractive index material. This approach allows us to realize highly reproducible

and ultralow cost mirrors. The large difference in the refractive index of the two materials allows us to obtain reflectivity better than 98% with a small number of periods, and to obtain a wide stop band with a full width at half maximum (FWHM) of about 200 nm. Moreover, this permits growth of fully evaporated microcavities in a single step process.

As demonstrated, we have realized three different λ quantum microcavities with Pyrromethene 580 as the active material and increasing output coupler reflectivity. We obtained a FWHM of the mode as low as 1.9 nm and a cavity Q value of about 300 by using an eight period output coupler. Angular dependent reflectivity is measured to probe the cavity mode for different longitudinal wave numbers. The cavity uniformity, probed by mapping the reflectivity in different positions across the sample surface, is very good, despite the large sample dimensions (about 25 mm^2) and the absence of a rotating sample holder in the evaporation chamber.

The DBRs are realized by thermal evaporation of λ/4 stacks of TeO$_x$/LiF on a Corning 5049 glass substrate and are designed to show a maximum reflectivity at 580 nm. The refractive index of the two materials, determined by means of transmittance and reflectance spectra, is about 2.25 for TeO$_x$ and about 1.39 for LiF in the wavelength range of interest. The materials are almost completely transparent in the range from 330 nm to 5 μm, thus they can be used for realization of dielectric mirrors in the entire visible and infrared range. The evaporation temperature is 1140 K for LiF and 1006 K for TeO$_x$. The typical vacuum in the chamber during the growth is below 8×10^{-7} mbar. The thickness of the layers is monitored *in situ* by a quartz oscillator microbalance that maintains the growth rate almost constant at

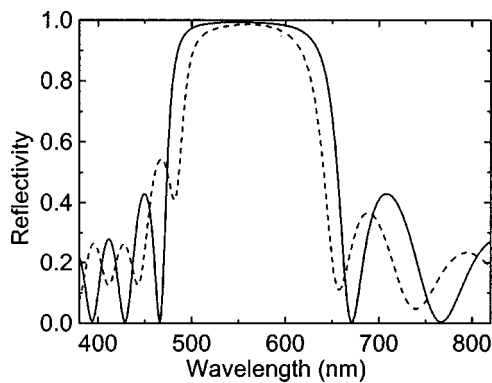[a]Electronic mail: marco.anni@unile.it

FIG. 1. Reflectivity of an eight period LiF/TeO$_x$ DBR calculated by the transfer matrix model (solid line) and experimental data from a real structure designed with the same parameters as the simulation. The peak reflectivity is 98.5% and the stop band is 160 nm wide.

FIG. 3. Reflectivity in the DBR stop band of the three cavities with six, seven, and eight period top mirrors. The spectra are shifted vertically for clarity. The reflectivity maximum value is 99.8%, 99.86%, and 99.94% for the six, seven, and eight output coupler cavities, respectively. The mode FWHM is 2.7 nm in the cavity with a six period top mirror, 2.3 nm in the cavity with a seven period top mirror, and 1.9 nm in the cavity with an eight period top mirror, corresponding to cavity Q values of 215, 270, and 300, respectively.

0.5 A s^{-1} to improve the film morphology. The reflectivity of an eight period mirror is shown in Fig. 1 (dashed line), together with the theoretical spectrum (solid line) calculated by the transfer matrix model. The maximum reflectivity value is about 98.5%, and the stop band is 160 nm wide. These values are slightly lower than the theoretical ones because the simulation does not take into account the absorbance of the $\lambda/4$ stacks.

As demonstrated we have realized three microcavities with output couplers of increasing reflectance. The complete structure of the three cavities is shown in Fig. 2. The bottom mirror is the same for all the cavities and consists on 8 TeO$_x$/LiF periods. The λ cavity is obtained by evaporating 200 nm of LiF on the bottom mirror, followed by a layer of Phyrromethene 580 about 4 nm in thickness, and by a second 200 nm thick layer of LiF. This structure allows us to obtain good overlap between the active material and the electric field antinode placed at the center of the cavity.[19,20] The structure is completed by evaporation of the top mirror, which consists of six, seven, or eight periods in the three different samples, respectively. We stress once more that the μ cavities were grown very simply by a sequential evaporation process in the same growth run. The substrate is kept at room temperature during growth in order to avoid crystallization or eventual thermal degradation of the active material.

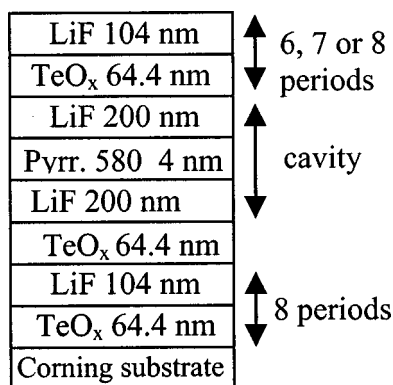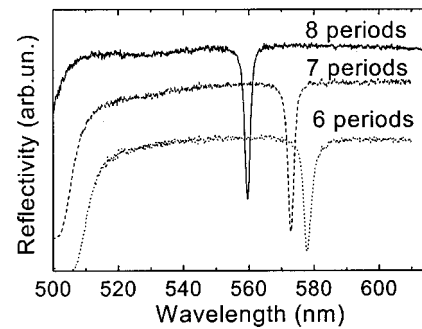The spectral properties of the cavities were probed by

reflectance measurements. The reflectivity spectra of the three cavities in the stop band spectral region are shown in Fig. 3. Two main features can be observed in the spectra as the output coupler reflectivity increases.

(1) The mode linewidth continuously decreases, from 2.7 nm for the six period top mirror to 1.9 nm for the eight period top mirror due to rising of the Q value of the cavity. The Q values of the cavities are 215, 270, and 300 for the six, seven, and eight period output coupler, respectively.

(2) The mode wavelength blueshifts, from 578 nm for a six period top mirror to 560 nm for an eight period top mirror. This is ascribed to cavity–mirror detuning, and is due to systematic variation of the lambda layer thickness arising from the nonuniform beam shapes over large areas, and to the phase matching effect inside the cavity, induced by the detuning.

The cavities show a bright photoluminescence (PL) emission, illustrated in Fig. 4 for the highest Q-value cavity, which demonstrates that the output coupler deposition does not damage the organic active material.

Angle dependent reflectivity measurements were performed to probe the spectral properties of the highest Q-value cavity for different longitudinal wave vectors. The

FIG. 2. Schematic layer structure of the three cavities realized using Pyrromethene 580 as the prototype organic material. The eight period bottom mirror is the same for the three samples, whereas the top mirror period number is varied between six and eight.
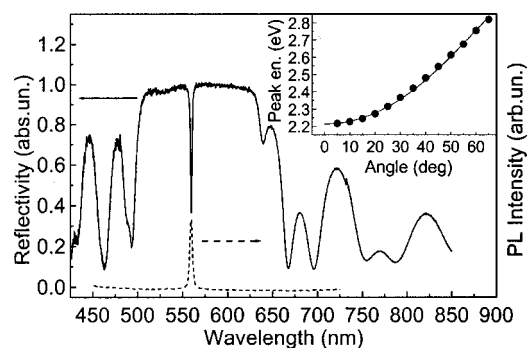

FIG. 4. PL spectrum (dotted line) and reflectivity spectrum (solid line) of the eight period top mirror cavity for normal incidence. The stop band FWHM is about 160 nm. Inset: Mode energy as a function of the angle of incidence. The continuous line is the best fit curve to a photon-like dispersion curve.
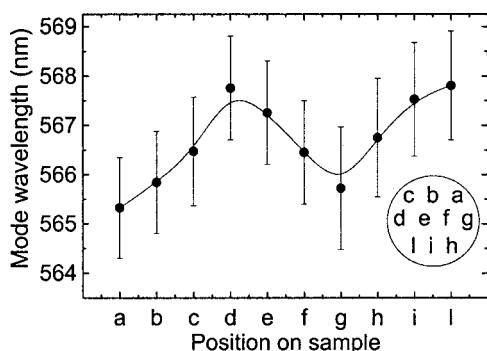
FIG. 5. Mode wavelength as a function of the position on the sample surface. The mode FWHM is taken as the error bar. The overall maximum variation of about 2.4 nm reflects the good uniformity of the sample despite dimensions of about 25 mm^2. Inset: Actual position of points a, b...,1 on the sample surface.

reflectivity spectrum of this cavity at normal incidence is shown in Fig. 4 and it displays a maximum value of 99.94% with a stop band FWHM of about 160 nm. The mode energy as a function of the incidence angle is shown in the inset of Fig. 4. As the incidence angle increases, the cavity mode shows a blueshift due to the increasing photon longitudinal wave vector. The angle dependence of the mode energy is reproduced well by photon-like dispersion for a cavity with mode energy at normal incidence of $E_0 = 2.212 \pm 0.001$ eV and an effective refractive index of $n = 1.451 \pm 0.002$. The n value, slightly higher than the LiF one, is mainly due to the presence of the organic layer whose refractive index, at the wavelength of the cavity, is complex and almost higher than the LiF value.

The uniformity of the cavity was checked by measuring the reflectivity in different zones along the sample surface (which has a circular shape 5.5 mm in diameter). The mode wavelength dependence on the position on the sample is shown in Fig. 5. The maximum mode wavelength variation is 2.4 nm, which is comparable with the mode linewidth. Moreover, the mode wavelength does not show random oscillations around or at the average value, showing instead a systematic redshift when moving across the sample from right to left (inset of Fig. 5) and a blueshift when moving in the opposite direction. This is connected to the nonuniform beam shape which induces systematic progressive variation of the layer thickness along the μ-cavity area and it can be removed by using a rotating sample holder to improve the thickness uniformity during evaporation.

In conclusion, we have described an approach to realize DBR dielectric mirrors based fully on thermal evaporation of LiF and TeO$_x$. This approach allows us to realize highly reproducible, wide stop band, high reflectivity mirrors. The wide stop band of our mirrors makes them particularly interesting for application to organic microcavities, since it allows one to obtain single peak luminescence despite the commonly seen broad luminescence spectrum of organic compounds. Moreover, the thermal evaporation technique is particularly suitable for organic material deposition due to its low cost, high controllability, and full compatibility with active material deposition, which allows single step fabrication of organic μ cavities. Our approach was tested by realizing high quality organic microcavities with mode linewidths as small as 1.9 nm, a Q value up to 300, and excellent uniformity over many mm^2. These results are relevant for application of LiF–TeO$_x$ DBRs in organic LEDs, flat panel displays, and laser resonators.

[1] G. Gu, G. Parthasarathy, P. E. Burrows, P. Tian, I. G. Hill, A. Kahn, and S. R. Forrest, J. Appl. Phys. **86**, 4067 (1999).
[2] P. E. Burrows, V. Khalfin, G. Gu, and S. R. Forrest, Appl. Phys. Lett. **73**, 435 (1998).
[3] D. G. Lidzey, M. A. Pate, D. M. Whittaker, D. D. C. Bradley, M. S. Weaver, T. A. Fisher, and M. S. Skolnick, Chem. Phys. Lett. **263**, 655 (1996).
[4] R. H. Jordan, L. J. Rothberg, A. Dodabalapur, and R. E. Slusher, Appl. Phys. Lett. **69**, 1997 (1996).
[5] A. Dodabalapur, L. J. Rothberg, R. H. Jordan, T. M. Miller, R. E. Slusher, and J. M. Phillips, J. Appl. Phys. **80**, 6954 (1996).
[6] J. Gruener, F. Cacialli, I. D. W. Samuel, and R. H. Friend, Synth. Met. **76**, 137 (1996).
[7] H. F. Wittmann, L. Gruener, R. H. Friend, G. W. C. Spencer, S. C. Moratti, and A. B. Holmes, Adv. Mater. **7**, 541 (1995).
[8] A. Dodabalapur, L. J. Rothberg, T. M. Miller, and Kwock Appl. Phys. Lett. **64**, 2486 (1994).
[9] T. Tsutsui, N. Takada, S. Saito, and E. Ogino, Appl. Phys. Lett. **65**, 1868 (1994).
[10] M. A. Diaz-Garcia, F. Hide, B. J. Schwartz, M. D. McGehee, M. R. Andersson, and A. J. Heeger, Appl. Phys. Lett. **70**, 3191 (1997).
[11] N. Tessler, G. J. Denton, and R. H. Friend, Nature (London) **382**, 695 (1996).
[12] D. G. Lidzey, D. D. C. Bradley, T. Virgili, A. Armitage, M. S. Skolnick, and S. Walker, Phys. Rev. Lett. **82**, 3316 (1999).
[13] T. Virgili, D. G. Lidzey, D. D. C. Bradley, G. Cerullo, S. Stagira, and S. De Silvestri, Appl. Phys. Lett. **74**, 2767 (1999).
[14] D. G. Lidzey, D. D. C. Bradley, M. S. Skolnick, T. Virgili, S. Walker, and D. M. Whittaker, Nature (London) **395**, 53 (1998).
[15] A. Arena, S. Patanè, G. Saitta, S. Savasta, R. Girlanda, and R. Rinaldi, Appl. Phys. Lett. **72**, 2571 (1998).
[16] T. Granlund, M. Theander, M. Berggren, M. Andersson, A. Ruzeckas, V. Sundstrom, G. Bjork, M. Granstrom, and O. Inganas, Synth. Met. **102**, 1038 (1999).
[17] A. Convertino, A. Valentini, and R. Cingolani, Appl. Phys. Lett. **75**, 322 (1999).
[18] M. Allegrini, A. Arena, M. Labardi, G. Martino, R. Girlanda, C. Pace, S. Patanè, G. Saitta, and S. Savasta, Appl. Surf. Sci. **142**, 603 (1999).
[19] T. Yamauchi, Y. Arakawa, and M. Nishioka, Appl. Phys. Lett. **58**, 2339 (1991).
[20] M. S. Skolnick, T. A. Fisher, and D. M. Whittaker, Semicond. Sci. Technol. **13**, 645 (1998).